A New Rigid Origami Mechanism and Motion Analysis

Aoxiang Tian[1,a], Jun Liu[2,b], Li Zhang[3,c*]

[a]Tax1105@163.com, [b]juneforjob@163.com, [c*]zlmse@hust.edu.cn

[1]School of Mechanical Science and Engineering Huazhong University of Science and Technology Wuhan, China
[2]Wuhan Second Ship Design and Research Institude Wuhan, China
[3]School of Mechanical Science and Engineering Huazhong University of Science and Technology Wuhan, China

Abstract—A new type of rigid origami mechanism is proposed in this paper, its combination mode is specified, and the calculation formula of the number of folding modes is given. Nine-plate rigid origami mechanism is one of the expressions of the new type of rigid origami mechanism. This paper takes the nine-plate rigid origami mechanism as an example, the Jacobian matrix method is used to calculate the degree-of-freedom (DOF) of the mechanism, and its kinematic model is established in the Cartesian coordinate system. The variation function of the dihedral angle of the nine-plate rigid origami mechanism with respect to the driving angle during the folding process was calculated, and the variation law of the dihedral angle during the folding process was obtained. The rigid origami mechanism has certain application potential in mechanical engineering fields such as underwater folding equipment and space scaling machinery.

Keywords-rigid origami mechanism; DOF calculation; kinematics model

1 Introduction

The origami mechanism is a unique mechanism that can convert 2D materials, such as plane paper, into a particular 3D shape by folding [1]. The rigid origami mechanism is an important branch of the origami mechanism. The rigid origami mechanism only rotates along the crease during the folding process, and does not bend and stretch [2]. The spatial folding motion of origami mechanisms is vibrant, which extends its applications in materials science [3,4], biology [5], and mechanical engineering [6]. Among them, the application in the field of mechanical engineering is mainly reflected in satellite antennas [7,8], solar cells [9], medical devices [10], folding robots [11], and so on.

The degree of freedom (DOF) of the origami mechanism represents the number of prime mover required for the mechanism to generate a determined motion. The DOF of the stated mechanism is usually obtained according to the Grübler-Kutzback criterion. However, for some complex mechanisms, such as masts, it often gives an incorrect DOF of less than 1. In order to solve this problem, Dai JS et al. introduced the screw theory to evaluate the mobility of such mechanisms, and the scissor-like element (SLE) multi-loop foldable mechanism is used to

IDEE 2023, November 24-26, Zhengzhou, People's Republic of China
Copyright © 2024 EAI
DOI 10.4108/eai.24-11-2023.2343448

verify the effectiveness of the theory [12]. Nagaraj et al. proposed a numerical algorithm to evaluate the mobility of pantograph masts by calculating the constrained Jacobian matrix [13]. Cai JG et al. extended this method to calculate the DOF of origami mechanisms [14], the accuracy of this method is better than that of Grübler-Kutzback method and its more suitable for computer simulation. This paper uses Cai JG et al 's method to calculate the DOF of origami mechanism.

In this paper, a new type of rigid origami mechanism is proposed. According to the combination of rigid origami mechanisms proposed, a series of rigid origami mechanisms including four-plate origami mechanisms and nine-plate rigid origami mechanisms can be constructed. In order to explore the motion mode of the new rigid origami mechanism, the motion analysis of the nine-plate rigid origami mechanism was carried out. The Jacobian matrix method is used to analyze its DOF, and its kinematics model is established in the Cartesian coordinate system. Finally, the variation of each dihedral angle during the folding process is obtained.

2 A New Type of Rigid Origami Mechanism

Two equilateral triangles and two isosceles triangles are combined, as shown in Fig. 1. Assuming all triangles are rigid triangles, a four-plate rigid origami mechanism is formed. It is also assumed that point B is fixed, so ABF and BCD rotate inward around point B synchronously in the plane where it is located, and folding can occur. Point E will move away from the plane as it folds.

Since the combination of two rotation directions of the hinges BF, BD, and BE can meet the folding of the four-plate rigid origami mechanism when folding begins from the tile state, the four-plate rigid origami mechanism has two folding patterns, as shown in Fig. 2. The " mountain " crease in the figure is represented by a solid line, and the " valley " crease is represented by a dotted line.

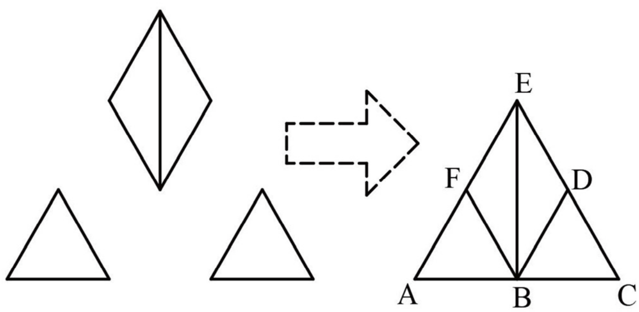

Figure 1 Combination method of four-plate rigid origami mechanism

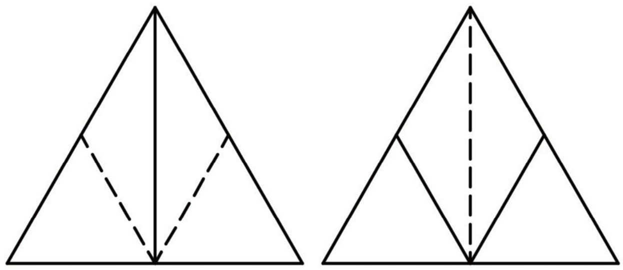

Figure 2 Two folding patterns of four-plate rigid origami mechanism

Using the same combination method, a nine-plate rigid origami mechanism (Fig. 3) can also be obtained. Assume that points B and C are fixed, so that ABI and CDE rotate inward around points B and C synchronously in the plane where they are located, a similar folding can also occur.

Similarly, since all hinges have four combinations of rotation directions to meet the folding of the nine-plate rigid origami mechanism when folding from the tile state, the nine-plate rigid origami mechanism has four folding methods, as shown in Fig. 4.

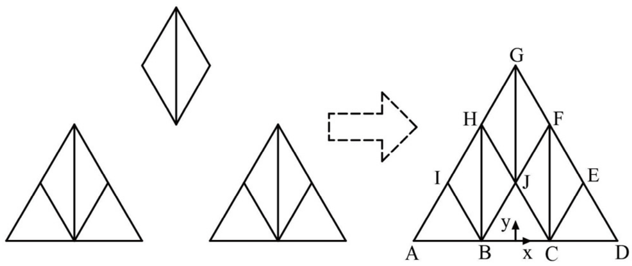

Figure 3 Combination method of nine-plate rigid origami mechanism

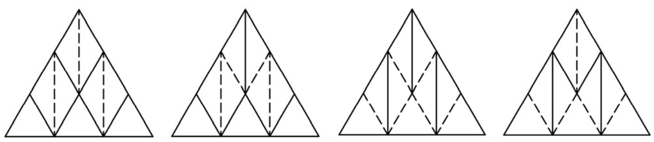

a. Pattern 1 b. Pattern 2 c. Pattern 3 d. Pattern 4

Figure 4 Four folding patterns of nine-plate rigid origami mechanism

Using the similar method, a rigid origami mechanism containing $n^2 \left(n \in N^+\right)$ triangular plates can be combined. The relationship between the number of folding patterns(m) of rigid origami mechanism and the number of plates(n) is:

$$m = 2^{(n-1)} \quad (1)$$

3 Motion Analysis of Nine-Plate Rigid Origami Mechanism

The nine-plate rigid origami mechanism is a form of expression of the new rigid origami mechanism， and the motion characteristics of the new rigid origami mechanism can be better reflected by the folding process of the nine-plate rigid origami mechanism. Therefore, taking the nine-plate rigid origami mechanism as an example, the folding process is explored, the DOF is analyzed, and the kinematic model of the folding pattern 1 of the nine-plate rigid origami mechanism is established.

3.1 Dof Analysis

The Jacobian matrix method is used to calculate the DOF of rigid origami mechanisms. The system constraint equation can be obtained by constructing the rigid constraint equation, joint constraint equation, and boundary condition of the rigid origami mechanism. The Jacobian matrix is the derivative of the system constraint equation with respect to time. The null space dimension of the Jacobian matrix represents the number of degrees of freedom of the rigid origami mechanism.

Firstly, the coordinate system in terms of the x, y, and z axes is established. The x and y coordinate axes are shown in Fig. 3, and the z coordinate axis can be determined according to the right-hand rule. For the convenience of calculation, the side lengths of the equilateral triangle ABI, CDE, and BCJ are all set to 1, and the coordinates of each node of the nine-plate rigid origami mechanism are provided in Table 1.

Table 1 The coordinates of each node of nine-plate rigid origami mechanism

Node	**A**	**B**	**C**	**D**	**E**
x	-1.50	-0.50	0.50	1.50	1.00
y	0	0	0	0	0.87
z	0	0	0	0	0
Node	**F**	**G**	**H**	**I**	**J**
x	0.50	0	-0.50	-1.00	0
y	1.73	2.60	1.73	0.87	0.87
z	0	0	0	0	0

The rigid constraint equation represents the nine triangular rigid plates that combine the nine-plate rigid origami mechanism. During the folding process, the shape of the triangular rigid plate does not change, which means that the length of each side of the triangle does not change:

$$\begin{cases} l_{AB}, l_{BC}, l_{CD}, l_{DE}, l_{EF}, l_{FG}, l_{GH}, l_{HI}, l_{IA}, l_{BI}, l_{BJ}, l_{CJ}, l_{CE}, l_{JH}, l_{JF} = 1 \\ l_{BH}, l_{CF}, l_{JG} = 1.73 \end{cases} \quad (2)$$

In the formula, l_{ij} represents the distance between the node i and the node j, and the equation composed of the three-dimensional coordinates of each node and the side length of each triangular rigid plate during the folding process can be obtained, which is the rigid constraint equation of the nine-plate rigid origami mechanism:

$$\begin{cases}(x_A-x_B)^2+(y_A-y_B)^2+(z_A-z_B)^2=l_{AB}{}^2\\(x_B-x_C)^2+(y_B-y_C)^2+(z_B-z_C)^2=l_{BC}{}^2\\\cdots\\(x_J-x_G)^2+(y_J-y_G)^2+(z_J-z_G)^2=l_{JG}{}^2\end{cases}\qquad(3)$$

The joint constraint of the folding origami mechanism represents the connection between the rigid plates, which can be regarded as two spherical joint constraints arranged at both ends of the crease. If the two adjacent triangular rigid plates are always in a coincidence state at a certain point during the folding process, the spherical joint constraints of the two plates here are automatically satisfied. When the nine-plate rigid origami mechanism satisfies the rigid constraint equation, its joint constraints are inevitably satisfied.

Boundary conditions refer to the other additional constraints. In this case, points B and C are fixed, and ABI and CDE are restricted to rotate symmetrically relative to BCJ. The boundary conditions are given below:

$$\begin{cases}x_B=-0.5\\y_B=z_B=\mathrm{y}_C=z_C=z_J=0\\z_A=z_I=z_D=z_E=0\\y_A-y_D=0\end{cases}\qquad(4)$$

In short, the system constraint equation of the nine-plate rigid origami mechanism can be rewritten as:

$$f_j\left(x_1\cdots x_n,y_1\cdots y_n,z_1\cdots z_n\right)=0,j=1,2\cdots m\quad(5)$$

In the formula, “ m ” represents the number of constraint equations, and “ n ” represents the number of joints of nine-plate rigid origami mechanism.

The system constraint equation of the folding process of the ideal origami mechanism is a set of functions about time. Deriving it with respect to time, the Jacobian matrix equation can be obtained.

$$[B]\dot{X}=0\qquad(6)$$

The Jacobian matrix B in the formula:

$$B=\begin{pmatrix}\frac{\partial f_1}{\partial x_1}&\cdots&\frac{\partial f_1}{\partial x_n}\\\cdots&\ddots&\cdots\\\frac{\partial f_m}{\partial x_1}&\cdots&\frac{\partial f_m}{\partial x_n}\end{pmatrix}\qquad(7)$$

If the dimension of the null space of the Jacobian matrix B is greater than 1, then there will be a nonzero vector, and the mechanism has DOF in the direction of this nonzero vector. Therefore, the dimension of the null space of the Jacobian matrix B represents the DOF of the nine-plate rigid origami mechanism.

There are 29 constraint equations and 30 coordinate variables in the nine-plate rigid origami mechanism. Therefore, the Jacobian matrix of the stated example is a 29×30 matrix. Importing the matrix into MATLAB, the null space dimension of the matrix turns out to be 1, which means that the spatial DOF of the nine-plate rigid origami mechanism is 1.

3.2 The Establishment Of The Kinematics Model

The motion theory of the origami mechanism can be described in the Cartesian coordinate system. The Cartesian coordinate system is fixed on each relatively moving object to represent the motion of the object. The matrix describes the rotation and translation transformation of the adjacent Cartesian coordinate system, and then the multiple transformation matrices are multiplied in order to establish the kinematics model of the origami mechanism.

The Cartesian coordinate system can be established by fixing each coordinate system to the triangle corresponding to the number of the nine-plate rigid origami mechanism, as shown in Fig. 5 [15].

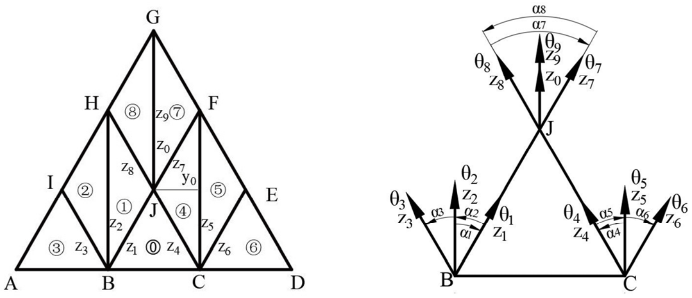

a. Number of the rigid plate b. Cartesian coordinate system

Figure 5 Nine-plate rigid origami mechanism

A list of the pose transformation matrix of adjacent triangles and their coordinate transformation parameters are given in Table 2.

Table 2 The pose transformation matrix of adjacent triangles and their coordinate transformation parameters

Pose transformation matrix	Relative to the X axis		Relative to the X axis		Relative to the X axis	
	α	***a***	***γ***	***b***	***θ***	***c***
$^{1}T_0$	$-\pi/6$	0	0	0	θ_1	-1.00
$^{2}T_1$	$\pi/6$	0	0	0	θ_2	0
$^{3}T_2$	$\pi/6$	0	0	0	θ_3	0
$^{4}T_0$	$\pi/6$	0	0	0	θ_4	-1.00
$^{5}T_4$	$-\pi/6$	0	0	0	θ_5	0
$^{6}T_5$	$-\pi/6$	0	0	0	θ_6	0
$^{7}T_4$	$-\pi/3$	0	0	-0.87	θ_7	0.50
$^{8}T_1$	$\pi/3$	0	0	0.87	θ_8	0.50

Since the above pose transformation matrix only involves the rotation relative to the X-axis, the translation relative to the Y-axis, and the rotation and translation relative to the Z-axis, the general formula of the pose transformation matrix is:

$$
{}^{i}T_{j} = R(X,\alpha) * Trans(b) * R(Z,\theta) * Trans(c) = \begin{bmatrix} \cos\theta & -\sin\theta & 0 & 0 \\ \cos\alpha\sin\theta & \cos\alpha\cos\theta & -\sin\alpha & b\cos\alpha - c\sin\alpha \\ \sin\alpha\sin\theta & \sin\alpha\cos\theta & \cos\alpha & c\cos\alpha + b\sin\alpha \\ 0 & 0 & 0 & 1 \end{bmatrix} \quad (8)
$$

Then we can get the expression of a point on any triangle in any coordinate system, for example:

$$
{}^{3}T_{0} = {}^{1}T_{0} * {}^{2}T_{1} * {}^{3}T_{2} \quad (9)
$$

$$
{}^{8}T_{0} = {}^{1}T_{0} * {}^{8}T_{1} \quad (10)
$$

Since the nine-plate rigid origami mechanism has four folding patterns, different folding patterns correspond to different kinematic models. Taking the folding pattern 1 as an example, the function of the dihedral angle can be obtained according to the solid geometry relationship (Formulas (11) - (15)), which is brought into the pose transformation matrix to establish the kinematic model of the nine-plate rigid origami mechanism.

$$
\theta_1 = \theta_3 = \theta_4 = \theta_6 = \frac{\arccos\left[8\sqrt{3}\left(a - b^2\right)\right]}{-3\cot(\theta)} \quad (11)
$$

In the above formula, a and b are:

$$
\begin{cases} a = \sin\frac{\theta^2}{2} - \frac{\cot\frac{\theta^2}{2}}{16} - \frac{1}{16} \\ b = \sin\frac{\theta}{2} - \frac{1}{4\sin\frac{\theta}{2}} \end{cases} \quad (12)
$$

$$
\theta_2 = \theta_5 = 2\arcsin\left(2\arcsin\frac{\theta}{2}\right) \quad (13)
$$

$$
\theta_7 = \theta_8 = \pi - PQR - \theta_2 \quad (14)
$$

$$
\theta_9 = -2\arcsin\left[2\sqrt{3}\cos\left(\frac{\theta}{2} + \frac{\pi}{3}\right) - 1\right] \quad (15)
$$

The function image of each dihedral angle of the nine-plate rigid origami mechanism with respect to θ is shown in Fig. 6, and the value range of the independent variable θ is $[0, \pi/3]$. However, in the actual folding process, when θ decreases from $\pi/3$ to the inflection points of θ_7 and θ_8 functions shown in the figure, points F and H overlapped. Although, theoretically, it can still be folded, if the nine-plate rigid origami mechanism is materialized, it will interfere with the folding.

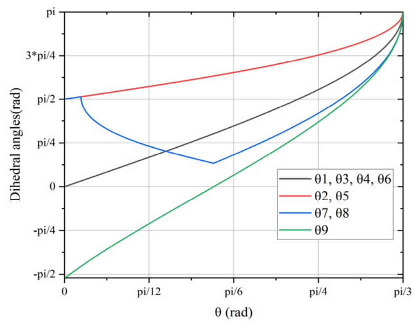

Figure 6 Function image of each dihedral angle of nine-plate rigid origami mechanism with respect to θ

4 Conclusions

In this paper, a new type of rigid origami mechanism is proposed, and the nine-plate rigid origami mechanism is a form of expression of it, which can represent its motion characteristics. For the nine-plate rigid origami mechanism, it is obtained that its DOF is 1 by calculating the null space dimension of the constructed Jacobian matrix, and its kinematic model is established, and the variation law of the dihedral angle during the folding process is analyzed. When the new rigid origami mechanism is folded, it will curl itself, reducing the length in the Y direction and increasing the length in the Z direction, which makes the whole more compact.

This basic rigid origami mechanism has certain application potential in space folding machinery. The plate structure of the rigid origami mechanism makes the overall rigidity of the tiled state weak, so the anti-deformation ability of the tiled state should be considered in practical application.

Acknowledgment: This work was supported by Provincial Teaching Research Project of Colleges and Universities in Hubei Province (2022039).

Aoxiang Tian: Conceptualization, Methodology, Investigation, Validation, Formal analysis and Writing, LI Zhang: Writing Instruction, provides language help, Jun Liu: Results and discussions.

Corresponding author: Li Zhang(zlmse@hust.edu.cn), ph. D. associate professor at School of Mechanical Science and Engineering, Huazhong University of Science and Technology, Wuhan, China.

References

[1] Chen, Y., Sareh, P., Yan, J., Fallah, A. S., Feng, J. (2019) An Integrated Geometric-Graph-Theoretic Approach to Representing Origami Structures and Their Corresponding Truss Frameworks. Journal of Mechanical Design, 141(9):1.

[2] Wang, K., Chen, Y. (2011). Folding a Patterned Cylinder by Rigid Origami. In P. Wang-Iverson, R. J. Lang, & M. YIM (Eds.), Origami 5. A K Peters/CRC Press. Massachusetts. 265-276.

[3] Dalaq, A. S., Khazaaleh, S., Daqaq, M. F. (2023) An origami-inspired design of highly efficient cellular cushion materials. Applied Materials Today, 32:101835.

[4] Liu, K., Li, P., Wang, Z. (2023) Buckling-regulated origami materials with synergy of deployable and undeployable features. International Journal of Mechanical Sciences, 247:108167.

[5] Kong, G. Z., Xiong, M. Y., Liu, L., et al. (2021) DNA origami-based protein networks: from basic construction to emerging applications. Chemical Society Reviews, 50(3):1846-1873.

[6] Yan, C., Yuanqing, G. (2023) Overview of origami kinematics. Advances in Mechanics, 53(1):154-197.

[7] Jape, S., Garza, M., Ruff, et al. (2020) Self-foldable origami reflector antenna enabled by shape memory polymer actuation. Smart Materials and Structures, 29(11):115011

[8] Georgakopoulos, S. V., Zekios, C. L., Sattar-Kaddour, et al. (2021) Origami Antennas. IEEE Open Journal of Antennas and Propagation, 2:1020-1043.

[9] Xu, Y., Ma, J., Liu, D., Xu, H., Cui, F., Wang, W. (2019) Origami system for efficient solar driven distillation in emergency water supply. Chemical Engineering Journal, 356:869-876.

[10] Zhao, W., Li, N., Liu, L., Leng, J., Liu, Y. (2022) Origami derived self-assembly stents fabricated via 4D printing. Composite Structures, 293:115669.

[11] Li, S., Stampfli, J. J., Xu, H. J., Malkin, E., Diaz, E. V., Rus, D., et al. (2019) A Vacuum-driven Origami "Magic-ball" Soft Gripper. Paper presented at the 2019 International Conference on Robotics and Automation (ICRA). 7401-7408.

[12] Dai, J. S., Li, D., Zhang, Q., Jin, G. (2004) Mobility analysis of a complex structured ball based on mechanism decomposition and equivalent screw system analysis. Mechanism and Machine Theory, 39(4):445-458.

[13] Nagaraj, B. P., Pandiyan, R., Ghosal, A. (2009) Kinematics of pantograph masts. Mechanism and Machine Theory, 44(4):822-834.

[14] Cai, J., Qian, Z., Jiang, C., Feng, J., Xu, Y. (2016) Mobility and Kinematic Analysis of Foldable Plate Structures Based on Rigid Origami. Journal of Mechanisms and Robotics, 8(6):064502.

[15] Chen, X., Feng, H., Ma, J., Chen, Y. (2019) A plane linkage and its tessellation for deployable structure. Mechanism and Machine Theory, 142:103605.